efficient resonant charge transfer, electrons are not able to hop from one SF_6 to another, again inhibiting rapid propagation of charge.

Conclusion

We have shown that many of the properties of the negative ion SF_6^- are not consistent with a structure resembling the parent neutral. The lack of photodetachment and the kinetic barrier associated with SF_6^- ion-molecule reactions are consistent with a highly distorted anionic structure. The autodetachment lifetime calculated from statistical rate theory implies that SF_6^- is much less tightly bonded than the parent neutral. While the model of a loose octahedral SF_6^- and the model of an ion-molecule association complex for SF_6^- are both consistent with these observations, we find the bonding changes required by the octahedral system difficult to rationalize. There are hints that other halogenated systems besides SF_6^- exhibit behavior which may be explained by similar models. Whether these models are a general phenomena or are specific to SF_6^- remains to be explored.

Acknowledgment. We are grateful to the National Science Foundation for support of this work and for fellowship support to P.S.D.

Note Added in Proof. Recent experimental[47] and theoretical[48] work supports an SF_6 electron affinity of roughly 1 eV. As noted, the statistical autodetachment lifetime is consistent with a "tight" SF_6^- if the SF_6 EA is this high, and the distorted octahedral model becomes acceptable. The complex model remains consistent as well.

The infrared multiphoton photochemistry of SF_6^- also suggests a distorted structure.[49]

(47) Streit, G. E. *J. Chem. Phys.*, submitted for publication.
(48) Hay, P. J. *J. Chem. Phys.*, in press.
(49) Drzaic, P. S.; Brauman, J. I. *Chem. Phys. Lett.* **1981**, *83*, 508.

Chloronium Ions as Alkylating Agents in the Gas-Phase Ion-Molecule Reactions with Negative Temperature Dependence

D. K. Sen Sharma and P. Kebarle*

Contribution from the Chemistry Department, University of Alberta, Edmonton, Alberta, Canada T6G 2G2. *Received June 12, 1981*

Abstract: The kinetics of the reactions $Me_2Cl^+ + B = MeB^+ + MeCl$ and $MeEtCl^+ + B = MeB^+$ or $(EtB^+) + EtCl$ (or MeCl) were studied with a pulsed-electron-beam, high-pressure mass spectrometer. At room temperature the rate constants were found to increase in the order B = benzene, toluene, isopropylbenzene, EtOH, Me_2O, Et_2O. At this point k became equal to the orbiting capture rate constant $k_L \approx 10^{-9}$ molecule^{-1} cm^3 s^{-1}. NH_3 and Me_3N were alkylated at orbiting capture rates. The temperature dependence of the rate constants for B = toluene, Me_2O, and Et_2O was examined. The rate constants were found to increase with decrease of temperature. This increase continued until the rate constants reached the magnitude of the orbiting rate constants k_L. The rates remained approximately independent of temperature below this temperature. At low temperatures the collision-stabilized Me_2Cl^+B and $MeEtCl^+B$ could be observed. The temperature dependence of the equilibrium $Me_2Cl^+ + toluene = (Me_2Cl\text{-}toluene)^+$ was measured and led to the corresponding $\Delta H°$ and $\Delta S°$. The reaction $Me_2Cl^+ + benzene = Me\text{-}benzene^+ + MeCl$ was found to have positive temperature dependence. On the basis of the above data it is suggested that the reactions $Me_2Cl^+ + B = MeB^+ + MeCl$ have an internal barrier in the potential energy of the reaction coordinate. This barrier protrudes above the energy level of the reactants ($Me_2Cl^+ + B$) for B = benzene. This leads to positive temperature dependence. For all other B, the top of the internal barrier lies below the level of the reactants and sinks lower, roughly in the order of increasing basicity of B. This leads to negative temperature dependence (toluene, isopropylbenzene, Me_2O, Et_2O). For B = NH_3, Me_2NH_2, Me_3N, the barrier is so low that the reactions have orbiting capture rates equal to k_L. Alkylation of bases B by chloronium ions like Me_2Cl^+ might have considerable utility in mass spectrometric analysis by chemical ionization. Ethers can be distinguished from alcohols and tertiary amines from primary and secondary amines. The alkylated ethers and the tertiary amines have no protic hydrogens and therefore do not form strongly hydrogen-bonded adducts.

Introduction

This work represents a continuation of studies of the gas-phase chemistry of halonium ions. Earlier work[1,2] provided binding energies $R^+\text{-}XR'$ from measurement of the equilibria $R^+ + XR' = (RXR')^+$. The present report deals with alkylation of bases B by alkylchloronium ions. An example of such a reaction is shown in eq 1. We have examined the methylation and ethylation

$$(CH_3)_2Cl^+ + (CH_3)_3N = (CH_3)_4N^+ + CH_3Cl \qquad (1)$$

of a number of π and n donor bases. Alkylbromonium and -chloronium ions are often used as alkylating agents in solution and have synthetic utility.[3] We thought it of interest to examine whether the same reactions occur in the gase phase. These reactions can have a certain utility in the gas phase, for example, as a convenient route to the preparation of tertiary oxonium and quaternary ammonium ions.

The rates of exothermic ion-molecule reactions in the gas phase are generally chemically featureless since the rate constants can be predicted from the Langevin or ADO orbiting capture rates.[4] These depend on reduced mass, polarizability, and dipole moment and are always close to $k_L \approx 10^{-9}$ molecule^{-1} cm^3 s^{-1}. Furthermore, there is only a very weak temperature dependence. The alkylation rates by chloronium ions, observed in the present work, showed very different behavior. Some reactions showed negative tem-

(1) Sen Sharam, D. K.; Kebarle, P. *J. Am. Chem. Soc.* **1978**, *100*, 5828.
(2) Sen Sharma, D. K.; Mesa de Hojer, S.; Kebarle, P., to be submitted for publication.
(3) Olah, G. A. "Halonium Ions"; Wiley: New York, 1975.
(4) "Gas Phase Ion Chemistry"; Bowers, M. D., Ed.; Academic Press: New York, 1979.

0002-7863/82/1504-0019$01.25/0

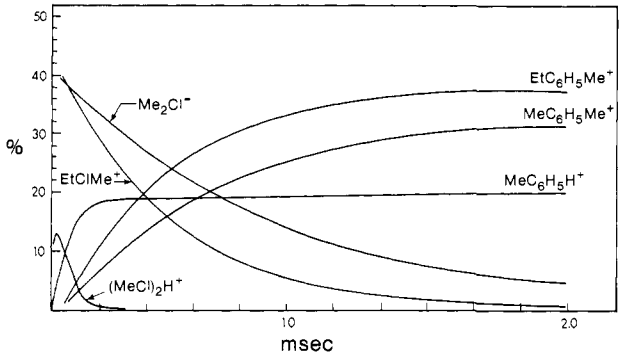

Figure 1. Ions observed after short electron pulse with reaction mixture: CH_4, 4 Torr; MeCl, 0.1 Torr; toluene, 1.5 mTorr; 32 °C. The major ions visible at short times, Me_2Cl^+ and $MeEtCl^+$, are formed by fast reactions 2–5. These ions alkylate toluene. Me_2Cl^+ leads to $MeC_6H_5Me^+$ while $MeEtCl^+$ leads exclusively to $EtC_6H_5Me^+$.

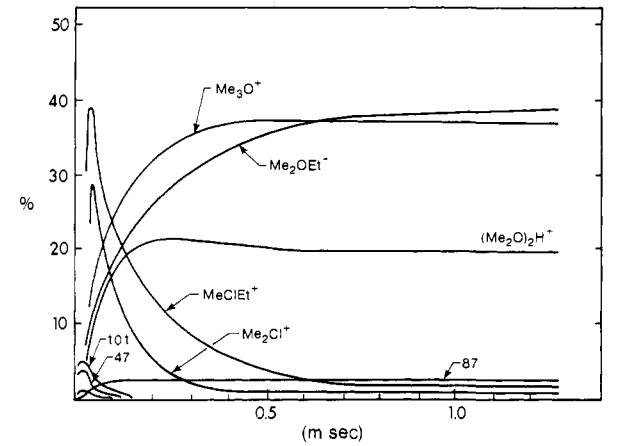

Figure 2. Ions observed with reaction mixture: CH_4, 4 Torr; MeCl, 25 mTorr; Me_2O, 0.22 mTorr; 28 °C. Me_2Cl^+ methylates the dimethyl ether, while $MeEtCl^+$ leads to Me_2OEt^+. Note that methylation by Me_2Cl^+ is faster than ethylation by $MeEtCl^+$ for Me_2O while the reverse was the case for toluene in Figure 1.

perature dependence. The rate constants increased with temperature decrease up to the point where they reached the (approximate) orbiting rates k_L. Others showed positive temperature dependence. Further, the reaction rates for different bases B showed also some dependence on exothermicity of the reaction. It has been our belief that negative temperature dependence with $k_{exp} < k_L$ is intimately connected with the nature of the potential energy of the reaction coordinate.[5]

We believe that the present system of reactions provides a very graphic and engaging example of the importance of internal barriers on the temperature dependence of the rate constants.

Experimental Section

The measurements were made with a pulsed-electron-beam, high-ion-source pressure, mass spectrometer. The experimental conditions and procedures were similar to those used in the earlier work on chloronium ions.[1,2]

The rate constants for the alkylation reactions were determined from the time dependence of the normalized ion intensities, i.e., results like those shown in Figures 1–5. The pseudo-first-order rate constant $\nu = k[B]$ for the reaction, $C^+ + B \rightarrow D^+ + E$, was generally determined from plots like that shown in Figure 6B. This plot is based on the equation shown below.

$$C^+ + B \xrightarrow{\nu} D^+ + E$$

$$[D^+]_t - [D^+]_0 = \nu \int_0^t [C^+]\, dt$$

(5) Kebarle, P. In "Interactions Between Ions and Molecules"; Ausloos, P., Ed.; Plenum: New York, 1975; p 470. Hiraoka, K.; Kebarle, P. *Can. J. Chem.* **1980**, *58* 2262.

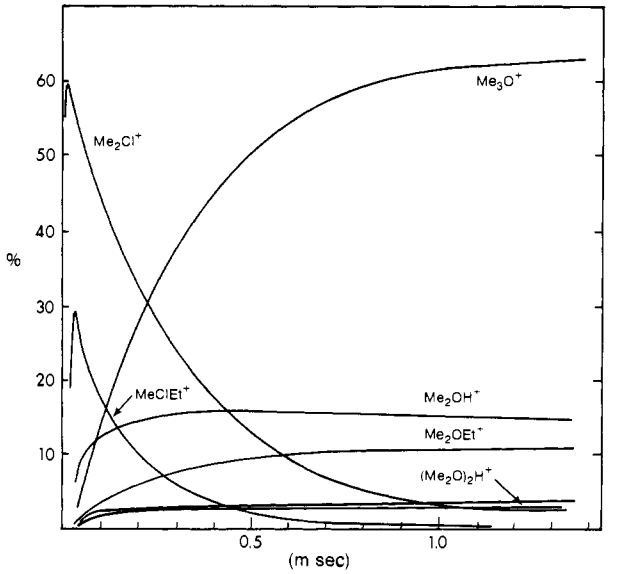

Figure 3. Ions observed with reaction mixture: CH_4, 4 Torr; MeCl, 220 mTorr; Me_2O, 1.1 Torr; 318 °C. At this higher temperature Me_3O^+ is the major product. The low yield of Me_2OEt^+ is due to decomposition of $MeClEt^+$ t Et^+ + MeCl at higher temperature. The Et^+ protonates MeCl and this leads to Me_2Cl^+ via reaction 3.

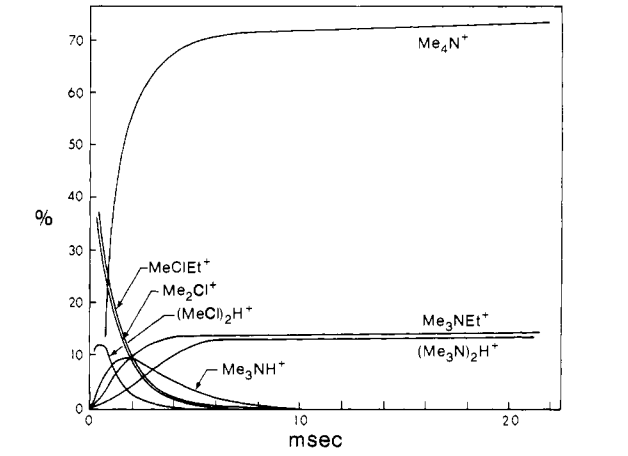

Figure 4. Ions observed with reaction mixture: CH_4, 4 Torr; MeCl, 0.1 Torr; Me_3N, 0.5 mTorr; 32 °C. Me_2Cl^+ methylates the base Me_3N. $MeEtCl^+$ also leads largely to methylation although Me_3NEt^+ is also formed but as a minor product. With the weaker bases toluene and ether, $MeEtCl^+$ produced only ethylation.

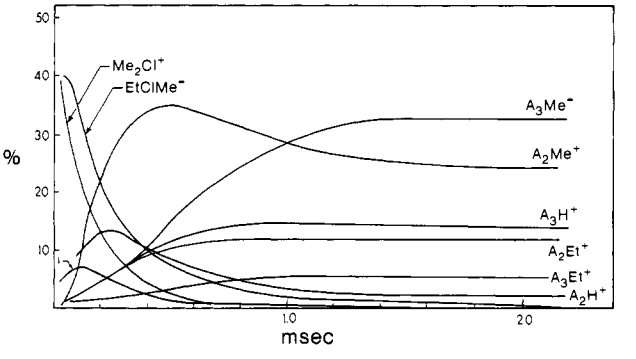

Figure 5. Ions observed with reaction mixture: CH_4, 4 Torr; MeCl, 0.1 Torr; NH_3 = A, 0.5 mTorr. Methylation by $EtMeCl^+$ is again favored with this strong base. Another effect is also of interest. Alkylation of Me_3N leads to a quaternary ammonium ion which has no protic hydrogens and cannot form hydrogen-bonded adducts (see Figure 4). On the other hand, ammonia and primary and secondary amines, after alkylation, have strongly protonic hydrogens and this leads to hydrogen-bonded association products: $MeNH_3^+(NH_3)_n = A_{n+1}Me^+$ and the corresponding $A_{n+1}Et^+$.

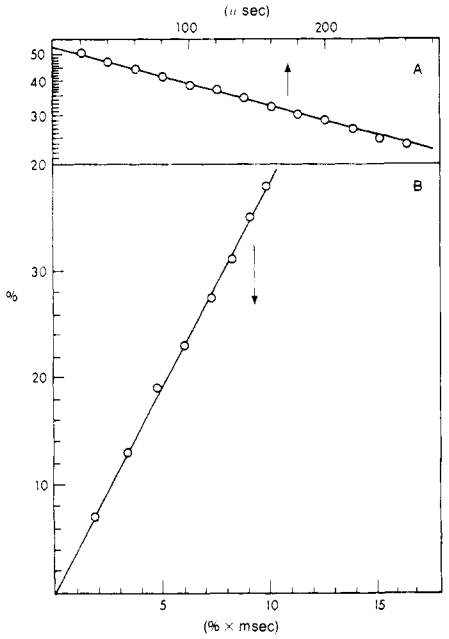

Figure 6. Rate constant determination plots; data from Figure 3 are used. Plot A shows ln $[Me_2Cl^+]$ vs. reaction time. The slope $\nu = k_7[Me_2O]$ leads to $k_7 = 1.7 \times 10^{-10}$ molecule^{-1} cm^3 s^{-1}. The plot shown in B involves $[Me_3O^+]$ vs. $\int_0^t [Me_2Cl^+]\,dt$ determined by graphical integration. The slope $\nu = k_7[Me_2O]$ leads to $k_7 = 2.1 \times 10^{-10}$ molecule^{-1} cm^3 s^{-1}. The result from plot B giving a somewhat larger k_7 is the more accurate one. The equation for plot B is given in the Experimental Section. This plot takes into account that Me_2Cl^+ is continually produced by the reverse of reaction 4 followed by reactions 5 and 3.

The integral at different times t was obtained by graphical integration of the area under the curve for $[C^+]$. The plot in Figure 6B is valid also when C^+ is formed by some reaction, while at the same time it reacts with B. When C^+ is not created by any reaction and reacts only with B, the conventional ln $[C^+]$ vs. t plot can also be used; see Figure 6A.

Results and Discussion

a. Reaction Mechanisms and Rate Constants of Alkylation Reactions. The ion intensities observed in some typical runs are shown in Figures 1–5. All these experiments were made with reaction mixtures consisting of methane as major gas at 4 Torr, and minor components MeCl and B at known pressures in the range: MeCl ~100 mTorr, B ~1 mTorr.

The kinetics by which the reactant ions Me_2Cl^+ and $MeClEt^+$ are formed in mixtures containing only methane and MeCl were described in our earlier publication.[1] These reactions are shown below. CH_5^+ and $C_2H_5^+$ are the ultimate ions resulting from

$$CH_5^+ + MeCl = MeClH^+ + CH_4 \quad (2)$$

$$MeClH^+ + MeCl = Me_2Cl^+ + HCl \quad (3)$$

$$Et^+ + MeCl + CH_4 = EtClMe^+ + CH_4 \quad (4)$$

$$Et^+ + MeCl = C_2H_4 + MeClH^+ \quad (5)$$

$$MeClH^+ + MeCl + CH_4 = (MeCl)_2H^+ + CH_4 \quad (6)$$

electron impact ionization and ion–molecule reactions of methane. Reactions 2–4 are fast for the chosen reaction mixtures and lead to the desired Me_2Cl^+ and $MeClEt^+$ in less than 50 μs after the ionizing pulse. In the presence of a base B, at concentration much lower than that of MeCl, reactions 7–9 occur. These reactions

$$Me_2Cl^+ + B = MeB^+ + MeCl \quad (7)$$

$$MeClEt^+ + B = EtB^+ + MeCl \quad (8a)$$

$$MeClEt^+ + B = MeB^+ + EtCl \quad (8b)$$

$$(Me_2Cl)_2H^+ + B = BH^+ + 2MeCl \quad (9)$$

$$Et^+ + B = C_2H_4 + BH^+ \quad (10)$$

Table I. Rate Constants and Thermochemistry

reaction	$10^{10}k^a$	$-\Delta H^b$	PA(B)^c
$Me_2Cl^+ + C_6H_6 = MeC_6H_6^+ + MeCl$	0.02	33	185.4
$MeEtCl^+ + C_6H_6 = EtC_6H_6^+ + MeCl$	>0.02	41	185.4
$Me_2Cl^+ + MeC_6H_5 = MeC_6H_5Me^+ + MeCl$	0.5	~34	193.7
$MeEtCl^+ + MeC_6H_5 = MeC_6H_5Et + MeCl$	0.9		193.7
$Me_2Cl^+ + i\text{-}PrC_6H_5 = i\text{-}PrC_6H_5Me^+ + MeCl$	1.2		~195
$MeEtCl + i\text{-}PrC_6H_5 = i\text{-}PrC_6H_5Et^+ + MeCl$	3.0		~195
$Me_2Cl^+ + EtOH = MeEtOH^+ + MeCl$	4.8	27	191.1
$MeEtCl^+ + EtOH = EtOH^+ + MeCl$	2.0	26	191.1
$Me_2Cl^+ + Me_2O = Me_3O^+ + MeCl$	10.5	31	193.8
$MeEtCl^+ + Me_2O = Me_2OEt^+ + MeCl$	5.0		193.8
$Me_2Cl^+ + Et_2O = Et_2OMe^+ + MeCl$	14.8		202.3
$MeEtCl^+ + Et_2O = Et_3O^+ + MeCl$			202.3
$Me_2Cl^+ + NH_3 = MeNH_3^+ + MeCl$	7.5	43	207.5
$MeEtCl^+ + NH_3 = EtNH_3^+ + MeCl$	1.6	39	207.5
$MeEtCl^+ + NH_3 = MeNH_3^+ + EtCl$	4.0		
$Me_2Cl^+ + Me_3N = Me_4N^+ + MeCl$	11.7	~64	228.3
$MeEtCl^+ + Me_3N = Me_3NEt^+ + MeCl$	4.0		228.3
$MeEtCl^+ + Me_3N = Me_4N^+ + EtCl$	7.0		
$Me_2Cl^+ + toluene = (Me_2Cl\ toluene)^+$	$\Delta S^\circ = -22$ cal K^{-1} mol^{-1}	12.2	

[a] Rate constant at 305 K (molecule^{-1} cm^3 s^{-1}). [b] Enthalpy change of reaction in kcal/mol. For B = benzene, alkylbenzene, alcohols, ammonia, and primary and secondary amines, ΔH can be evaluated from the proton affinities of the methylated or ethylated B, and DH° (Me^+-ClMe) ≈ 64.2 kcal/mol,[2] DH° (Et^+-ClMe) = 30.7 kcal/mol.[1,2] For B = Me_2N, ΔH cannot be evaluated directly since $\Delta H_f(Me_3O^+)$ and $\Delta H_f(Me_4N^+)$ are not available. These values were estimated from progressive changes in DH° (Me^+-B), with methyl substitution in B: Me^+-OH_2 = 71.9; Me^+-OHMe ≈ 85.4; Me^+-OMe_2 ≈ 95 (estd); Me^+-NH_3 = 107.2; Me^+-NH_2Me = 119.7; Me^+-$NHMe_2$ = 125.3, Me^+-NMe_3 ≈ 128 kcal/mol (estd). [c] Proton affinities for B, BMe, BEt from Franklin[16] and Lau,[17] adjusted to PA(NH_3) = 207.5 kcal/mol and $\Delta H_f(t\text{-}C_4H_9^+)$ = 164 kcal/mol, $\Delta H_f(H^+)$ = 365.7 kcal/mol.

can be clearly followed in each of the runs shown in Figures 1–5. For example, in Figure 1 which gives results for B = toluene, one observes a decrease of Me_2Cl^+ and a corresponding increase of $MeC_6H_5Me^+$. Similarly there is a decrease of $MeClEt^+$ and a corresponding increase of $EtC_6H_5Me^+$. The shape of the curves clearly indicates that reaction 8b does not occur for B = toluene. The curves also show that the ethylation of toluene by $EtClMe^+$ (eq 8a) is faster than the methylation by Me_2Cl^+ (eq 7), i.e., that $k_7 < k_{8a}$.

The reactions for B = Me_2O are shown in Figure 2. Again, reaction 8b does not occur to any significant extent, but now the methylation (eq 7) is faster than the ethylation (eq 8a).

The reactions for B = Me_3N are shown in Figure 4. Clearly methylation rather than ethylation is the major result of the encounter of $MeClEt^+$ with this base; i.e., reaction 8b, which did not occur with the weaker bases, is the major process for the strong base Me_3N.

Rate constants for reactions 7, 8a, and 8b were determined from a number of runs at 32 °C with different bases. The method used for these determinations is described in the Experimental Section and one example is given in Figure 6. The rate constants are summarized in Table I. Examination of these results reveals the following trends. The rate constants for the alkylation reactions increase approximately with increase of the basicity of the base. The weakest bases examined were benzene, toluene and isopropylbenzene. The rate constants are much smaller than $k_L \approx 10^{-9}$ molecule^{-1} cm^3 s^{-1}. The alkylation of the weakest base benzene, is so slow that it was difficult to measure at room temperature. For toluene, the rate constants are much higher but still only $^1/_{20}$th of k_L. A further increase is observed for isopropylbenzene. The observed k increases again for the stronger bases EtOH, Me_2O, Et_2O and became approximately equal to k_L for the strongest bases NH_3 and Me_3N. Also, as noted earlier,

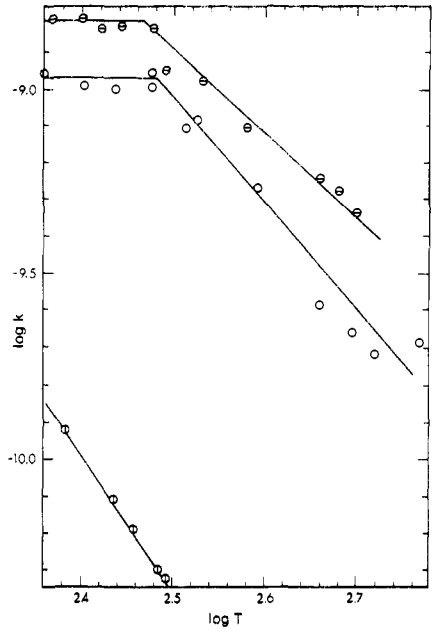

Figure 7. Temperature dependence of rate constants for reaction 7: ⊖, B = Et_2O; ○, B = Me_2O; ○, B = toluene. Region with strong temperature dependence obeys the empirical formula: $\log k = \log c - n \log T$. $c = 1.6 \times 10^{-3}$, $n = 2.435$ for Et_2O; $c = 7.8 \times 10^{-3}$, $n = 2.77$ for Me_2O; and $c = 0.11$, $n = 3.75$ for toluene. Plots of similar appearance were observed earlier by Field and co-workers for hydride transfer reactions.

an increase of basicity leads to increased methylation over ethylation. For the weakest bases, (8a) was faster than (7) and (8b) did not occur. For the ethers and ethyl alcohol, (7) is faster than (8a) but (8b) still does not occur; for ammonia and Me_3N, (7) is much faster than (8a) and also (8b) is favored over the ethylation (8a).

The temperature dependence of the reactions with benzene, toluene, isopropylbenzene, Me_2O, and Et_2O was studied in a series of runs. An example of such a run is given in Figure 3 which deals with Me_2O at 318 °C. A very much larger yield of Me_3O^+ relative to Me_2OEt^+ is observed at this temperature. At first glance, one might suppose that this is due to k_{8b} becoming larger than k_{8a} at higher temperature. A closer examination reveals a different cause. The dimer $(MeCl)_2H^+$ is unstable at higher temperature and more $MeClH^+$ is therefore available to produce Me_3O^+ via (3) followed by (7). Another change occurs also; at high temperature, reaction 4 becomes reversible (see Figure 3 in ref 1). Equilibrium 4 is strongly displaced toward $MeClEt^+$ in the run of Figure 3. Therefore, the Et^+ concentration was not recorded. Nevertheless, the presence of Et^+ has two consequences evident in Figure 3. Protonation of the base by the fast reaction 1 removes Et^+ and decreases the yield of Me_2OEt^+. Some Et^+ produces Me_3O^+ via reactions 5 followed by reactions 3 and 7.

Only the temperature dependence of k_7 was determined at high temperature, since the complications mentioned above render the determinations of k_8 difficult. The rate constants k_7 for toluene, isopropylbenzene, Me_2O, and Et_2O were found to decrease with temperature. Plots of $\log k_7$ vs. $\log T$ are shown in Figure 7 for Me_2O, Et_2O, and toluene. These results together with those in Table I will be examined in section c.

b. The Equilibrium Me_2Cl^+ + Toluene = $(Me_2Cl\text{-Toluene})^+$ and the Potential Energy Diagram for Reaction 7. There was a low-temperature limit below which the measurement of the rate constants for reaction 7 became complicated by the formation of collisionally stabilized complexes between the chloronium ion and the bases B. Complexes of B with Me_2Cl^+ were observed for B = Et_2O, Me_2O, and toluene, i.e., all three bases which were investigated at low temperature. For the ethers, the complex did not reach equilibrium with the Me_2Cl^+ ion; however, equilibrium 11 cold be observed with toluene. The formation of this stabilized

$$Me_2Cl^+ + \text{toluene} = (Me_2Cl\text{-toluene})^+ \qquad (11)$$

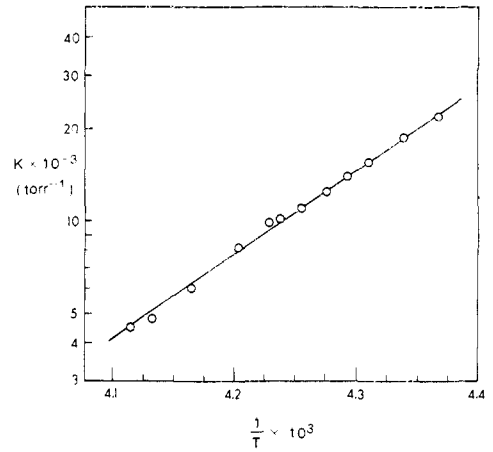

Figure 8. van't Hoff plot of equilibrium 11, Me_2Cl^+ + toluene = $(Me_2Cl\text{-toluene})^+$. Slope and intercept lead to: $\Delta H^\circ_{11} = -12.3 \pm 3$ kcal/mol and $\Delta S^\circ_{11} = -22 \pm 5$ cal K^{-1} mol^{-1}.

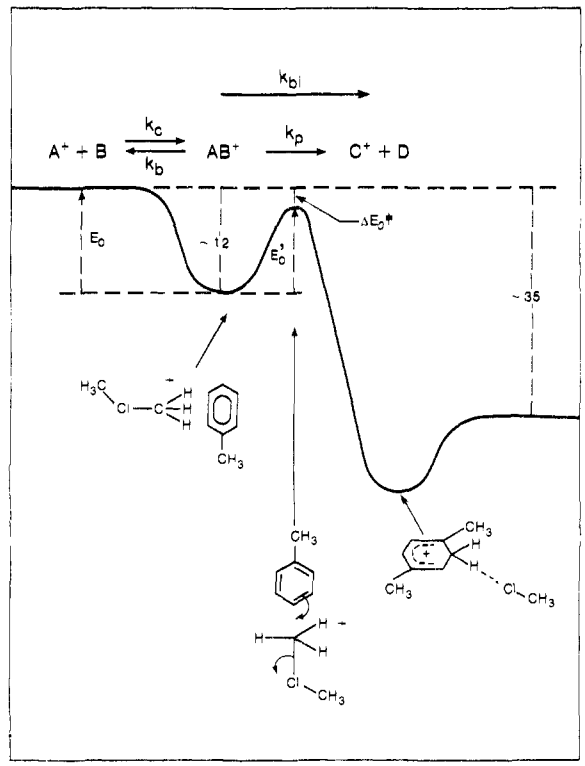

Figure 9. Change of potential energy along reaction coordinate for reactions 7. Potential drawn approximately to scale for B = toluene. The top of the internal barrier E_o' is believed to be above the energy level of the reactants ($A^+ + B$) for B = benzene. This leads to positive temperature dependence. For B = toluene, isopropylbenzene, EtOH, Me_2O, and Et_2O, the top of the barrier is below the level of the reactants sinking lower in the order above. This leads to negative temperature dependence. When the top of the barrier is so low that $k_p >> k_b$, then the reaction takes on the Langevin rate at all but the highest temperatures (B = NH_3, $MeNH_2$, Me_3N).

complex was at the expense of reaction 7 (B = toluene). The rate of (7) decreased while the complex concentration was building up to the equilibrium concentration. After the equilibrium concentration was reached, both Me_2Cl^+ and the complex decreased in constant proportion as the Me-toluene$^+$ increased. A van't Hoff plot of the equilibrium constant K_{11} is shown in Figure 8. The resulting ΔH°_{11} and ΔS°_{11} are given in Table I. The error of the measurement, ±3 kcal/mol and ±5 cal K^{-1} mol^{-1}, is estimated to be large because of the narrow range of temperatures over which K_{11} could be observed.

The data from equilibrium 11 together with the exothermicity for reaction 7 (B = toluene) were used to construct the potential

energy diagram shown in Figure 9. We have assigned to the collisionally stabilized complex the structure Me_2Cl^+-toluene and have assumed that this complex is separated from $MeC_6H_5Me^+$-ClMe by an internal energy barrier. The assumed structures of the two stable complexes and the transition complex are indicated in Figure 9.

A large barrier whose top is not much lower than the energy level of the reactants is indicated by the following considerations. The structures of the two stable complexes are very different. The large exothermicity of the reaction (35 kcal/mol) imposes a big difference in the zero-point energies of the two stable complexes. On the other hand, the transition state involves electronic and structural rearrangements which are likely to have a high-energy requirement. The minima of both stable complexes are expected to be shallow. The charge of Me_2Cl^+ is highly delocalized and bonding in Me_2Cl^+-toluene should be weak. The same is true for the charge delocalized toluene H^+ and the complex toluene H^+-ClMe. Considering the large exothermicity of the reaction the collisional stabilization of a complex $(Me_2Cl\text{-toluene})^+$ would be very unlikely in the absence of a large internal barrier. Thus the observation of equilibrium 11 in itself is strong evidence for the existence of a high internal barrier.

c. Temperature Dependence of Reactions 7: $Me_2Cl^+ + B = MeB^+ + MeCl$. A plot of the rate constants k_7 for B = Me_2O, Et_2O, and toluene which could be measured at low temperatures is shown in Figure 7. Two temperature regimes are exhibited. In the high-temperature region, the rate constant increases as the temperature decreases. This dependence can be expressed by the empirical eq 12. The increase of k with decrease of T continues

$$k = CT^{-n} \tag{12}$$

until the rate constant comes close to the value expected constant ($k_L \approx 10^{-9}$ molecule^{-1} cm^3 s^{-1}). Further lowering of the temperature has essentially no effect; i.e., the rate constants in this second temperature region follow the expected very slight temperature dependence for k_L.

As mentioned earlier, reaction 7 with B = toluene was very slow at 300 K. The results from equilibrium 11 for toluene (see preceding section) showed that there is a large internal barrier for this compound. The proton affinity of benzene is considerably lower than that for toluene (see Table I). Considering the possible nature of the transition complex (see Figure 9), one can expect that the top of the energy barrier for benzene should be higher than that of toluene. To form the transition state one has to pull an electron pair out of the aromatic ring and this should be easier with toluene than benzene. In fact, the top of the internal barrier for benzene might be so high that it protrudes above the energy of the reactants, i.e., above the dashed line in Figure 9. On basis of this reasoning, we examined the kinetics of reaction 7 (B = benzene) *above* room temperature. These experiments showed that the reaction has positive temperature dependence. Of course, positive temperature dependence is expected for an (internal) barrier protruding above the energy level of the reactants. For such a system an Arrhenius plot can be employed. Such a plot is shown in Figure 10. Also included in Figure 10 are Arrhenius plots of reaction 7 with B = toluene and isopropylbenzene, which have negative temperature dependence. These plots also lead to straight lines but with opposite slopes which lead to negative "activation" energies. These values probably cannot be directly identified with $\Delta E_0^{\ddagger}$ in Figure 9. However, they do indicate that $\Delta E_0^{\ddagger}$ is negative and quite small.

The temperature dependence for k_7 and B = benzene, toluene, and isopropylbenzene was interpreted above as a consequence of a progressive lowering of the top of the internal barrier (see Figure 9). The same concept can be applied also to the room-temperature results summarized in Table I. The observed increase of rate constants for the alkylation reactions in the order isopropylbenzene, EtOH, Me_2O, Et_2O, NH_3 coincides with an increase of the basicity of these compounds. The lone-pair orbitals of the oxygen and nitrogen bases are not only of higher energy, but also spatially more accessible to the electrophile. Thus a lowering of the energy barrier is expected for these bases.

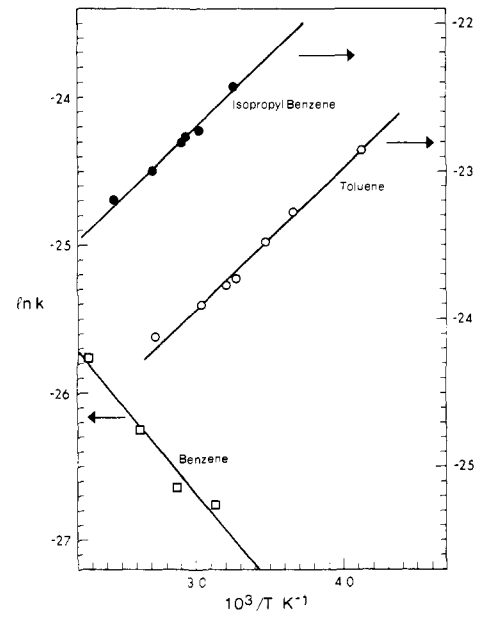

Figure 10. Arrhenius-type plots for rate constants k_7 for the reaction $Me_2Cl^+ + B = MeB^+ + MeCl$ for B = benzene (□), toluene (○), isopropylbenzene (●). Benzene has positive temperature dependence. Slope of plot leads to activation energy $E_A = 2.4$ kcal/mol. Preexponential factor $A = 0.95 \times 10^{-10}$ molecule^{-1} cm^3 s^{-1}. Toluene and isopropylbenzene have negative temperature dependence. Their slopes lead to exponential terms E/RT with $E = -2$ kcal/mol for both compounds. These values do not necessarily correspond to $\Delta E^{\ddagger}$ in Figure 9. The do, however, indicate that $\Delta E^{\ddagger}$ is negative.

As pointed out in section 2, ethylation was found to be faster than methylation when the basicity of the base was low (see Table I). Probably this trend is also related to the size of the internal barrier. It requires much less energy to detach Et^+ than Me^+ from the chloronium ion. For bases with relatively unavailable electron pairs (benzene), the ease of detachment of the alkyl cation will be relatively more important and lead to dominance of ethylation over methylation. Fore bases like NH_3 where the internal barriers should be very low, entropic factors should be more important and these could be favoring methyl over ethyl.

The reactions (7) where the rate constants $k_7 < k_L$ and the temperature dependence is negative can be treated with the RRKM theory for chemically activated systems.[6] Brauman et al.[7,8] have applied this theory to proton transfer and nucleophilic displacement gas-phase ion–molecule reactions. The treatment in ref 7 is particularly relevant to the reactions considered here. The potential energy diagrams are very similar. The exothermicity of the present reactions is considerably larger, but that is of no consequence to the application of the theory. The notation used by Brauman is shown in the potential energy diagram Figure 9. The chemically activated complex is AB. It is formed by $k_c \approx k_L$ and back decomposes by k_b. It forms products by k_p. The bimolecular rate constant which should be equal to the experimental rate constant is k_{bi} given by eq 13. When $k_p << k_b$, k_{bi}

$$k_{bi} = k_c k_p/(k_p + k_b) \tag{13}$$

becomes much smaller than k_L. This condition generally occurs when the barrier E_0' is large, even though $E_0 > E_0'$. This comes about because the entropy of the complex $AB^{\ddagger}$ at the barrier E_0' is generally much less favorable than the entropy of the loose complex corresponding to k_b, i.e., the internal energy levels for the back-reaction are more closely spaced than those for the forward reaction, at equal internal energy. (See Figure 2, Brauman[7]). Brauman[7] did not consider the temperature dependence of k_{bi}, but is is clear from the model used and eq 11 in

(6) Forst, W. "Theory of Unimolecular Reactions"; Academic Press: New York, 1973; p 200.
(7) Olmstead, W. N.; Brauman, J. I. *J. Am. Chem. Soc.* **1977**, *99* 4219.
(8) Farneth, W. E.; Brauman, J. I. *J. Am. Chem. Soc.* **1976**, *98*, 7891.

Brauman[7] that the temperature dependence generally will be negative. At low temperature, passage through the lower barrier E_0' is favored. At high temperatures, when the multiple paths corresponding to k_b can be fully utilized, k_b becomes larger than k_p, and k_{bi} decreases. A quantitative evaluation of k_{bi} at different temperatures is possible (see eq 11, Brauman[7]). Numerical input consisting of the vibrational frequencies, moments of inertia, and symmetry number for internal rotors for both transition states corresponding to k_p and k_b are required as well as the energy difference $E_0' - E_0$. These frequencies need not be too closely known (guessed) since the calculations are not too sensitive to the exact numerical input. However, very little is known about the present reaction systems involving the chloronium ions and bases like toluene; therefore, we did not attempt an RRKM calculation.

Meot-Ner, Field, et al.[9-13] have studied the kinetics and temperature dependence of hydride-transfer reactions (eq 14) involving

$$R_0^+ + RH = R_0H + R^+ \qquad (14)$$

alkyl cations R_0^+, R^+. These authors were the first to discover negative temperature dependence in ion–molecule reactions. The temperature dependence for many such reactions had the behavior pattern displayed by the present results in Figure 7; i.e. the rate constant increased with decrease of temperature until it came close to the Langevin–ADO values, where it became essentially temperature independent. To explain the negative temperature dependence of the reactions, Meot-Ner, Field, et al.[9-13] applied transition-state theory. Without giving any consideration to the possible shape of the potential energy of the reaction coordinate they assumed $\Delta E_0^{\ddagger} = 0$, justifying this by the statement that exothermic ion–molecule reactions have no energy barrier (i.e., no activation energy). The transition-state equation, with the assumption $\Delta E_0^{\ddagger} = 0$, can be approximately reduced to the same form as the experimentally observed eq 12. However, in TS theory $\Delta E_0^{\ddagger}$ stands not for an energy barrier but for the difference between the zero-point energy levels of the activated complex and reactants. Without specifying the potential energy of the activated complex on cannot select $\Delta E_0^{\ddagger}$. For the reactions in question $\Delta E_0^{\ddagger}$ is not 0 but negative. Therefore, we believe that the TST application by Meot-Ner, Field, et al. was incorrect. The negative temperature dependence of the hydride transfer reactions is a consequence of special properties of the potential energy diagram. A more detailed discussion claiming that the negative temperature dependence is due to internal barriers and low exothermicities of the reactions is given elsewhere.[14]

d. Utility of Alkylation Reactions in Chemical Ionization Analysis. The alkylation reactions 7 and 8 might have some utility to gas-phase-ion chemistry and ion analysis. Obviously they allow the preparation of alkylated bases like Me_4N^+ or Me_3O^+ which might be useful in thermochemical measurements. Also an analytical use in chemical ionization can be suggested. In chemical ionization one often identifies a given substrate compound B by forming a complex with an ion; for example, $NH_4^+ + B$ leads to BH^+ and BNH_4^+. Methylation by Me_2Cl^+ could be used for the same purpose. The reaction will lead to MeB^+. Alkylation by chloronium ions is a much milder process than the direct alkylation by the free alkyl cation. Therefore, the chloronium reaction is much cleaner; i.e., only alkylation occurs. On the other hand, the free alkyl cation may engage also in hydride abstraction or induce rearrangement and fragmentation.

Alkylation of oxygen and nitrogen bases is also a procedure which permits one to distinguish between ethers and alcohols and between tertiary and other amines. For example, methylation of ethers leads to tertiary oxonium ions which have no protic hydrogens and therefore no tendency to form strongly hydrogen-bonded adducts.[15] On the other hand, methylation of alcohols ROH leads to $ROHMe^+$ which can form $ROH{\cdot}ROHMe^+$ adducts. The same situation obtains for tertiary and other amines. For example, NH_3 after methylation forms adducts $MeNH_3{\cdot}(NH_3)_n^+$ (see Figure 5) while no corresponding adducts are observed for Me_4N^+ obtained from Me_3N (Figure 4). Experiments performed with EtOH led to adducts $MeEtOH^+(EtOH)_n$, while Me_2O and Et_2O did not form adducts after methylation or ethylation, (Figure 2).

Acknowledgment. This work was supported by the National Sciences and Engineering Research Council (NSERC) of Canada.

Registry No. Me_2Cl^+, 24400-15-5; $MeEtCl^+$, 24400-21-3; C_6H_6, 71-43-2; MeC_6H_5, 108-88-3; i-PrC_6H_5, 98-82-8; EtOH, 64-17-5; Me_2O, 115-10-6; Et_2O, 60-29-7; NH_3, 7664-41-7; Me_3N, 75-50-3.

(9) Solomon, J. J.; Meot-Ner, M.; Field, F. H. *J. Am. Chem. Soc.* **1974**, *96*, 3727.
(10) Meot-Ner, M.; Solomon, J. J.; Field, F. H.; Gerschinowitz, H. *J. Phys. Chem.* **1974**, *78*, 1773.
(11) Meot-Ner, M.; Field, F. H. *J. Am. Chem. Soc.* **1975**, *97*, 2014.
(12) Meot-Ner, M.; Field, F. H. *J. Chem. Phys.* **1976**, *64*, 277.
(13) Meot-Ner, M.; Field, F. H. *J. Am. Chem. Soc.* **1978**, *100*, 1356.
(14) Sen Sharma, D. K.; Magnera, T. F.; Kebarle, P., to be submitted for publication.
(15) Grimsrud, E. P.; Kebarle, P. *J. Am. Chem. Soc.* **1973**, *95*, 7939.
(16) Walder, R.; Franklin, J. L., *Int. J. of Mass Spectros. Ion Phys.* **1980**, *36*, 85.
(17) Lau, Y. K.; and Kebarle, P., unpublished work.